TITLE:

Rate of Heat Transfer between a Fluidized Bed and the Tube Wall at Higher Temperature

AUTHOR(S):

ASAKI, Zenjiro; NAGASE, Takao; AWAKURA, Yasuhiro; NAKANO, Isao; FUKUNAKA, Yasuhiro; KONDO, Yoshio

Rate of Heat Transfer between a Fluidized Bed and the Tube Wall at Higher Temperature

By

Zenjiro Asaki*, Takao Nagase**, Yasuhiro Awakura*, Isao Nakano***,
Yasuhiro Fukunaka* and Yoshio Kondo*

(Received August 7, 1971)

Synopsis

The heat transfer coefficient between a fluidized bed and the tube wall, h_w, was measured in the temperature range of 500° to 800°C. Quartz and fused alumina particles were fluidized in the air stream. The coefficient h_w was obtained between 70 and 800 kcal/m²·hr·°C. It increases with the flow rate of air. The effects of bed temperature and heat content and size of the particles on h_w were imperceptible.

By comparing the heat transfer coefficents obtained in this work with those at lower temperatures below 200°C, the difference between both coefficients was not significant.

1. Introduction

Knowledge of the heat transfer rate in a fluidized bed are indispensable for the kinetic studies on the reactions being carried out in the bed when they are associated with a large amount of heat evolved or consumed: the rate of heat removal or supply is needed in designing and operating the fluidized bed reactor.

With regard to the gas-solid fluidized bed, the following two types of heat transfer are important:

(1)   Heat transfer between fluidized bed and tube wall, and

(2)   Heat transfer between gas and fluidized particles.

It is intended in this work to contribute to the heat transfer problem of type (1) at higher temperatures. Though many works[1,2,3,4] have been done on the rate of heat transfer between fluidized bed and the tube wall, their results are rather divergent. And this divergency is thought to be caused by the different experimental conditions and methods of measurement employed. And Wen and Leva[5] tried to correlate the data of heat transfer coefficient between the fluidized bed and the wall obtained by the previous workers[2,3,4,6] and derived the following dimensionless equation,

* Department of Metallurgy, Kyoto Univ.
** Former Graduate Student, now with the Railway Technical Research Institute, JNR
*** Former Student, now with Research and Development Center, Sanyo Electric Co., Ltd.

$$\frac{h_w D_p}{k_g} = 0.16 \left(\frac{C_s \rho_s D_p{}^{1.5} g^{0.5}}{k_g} \right)^{0.4} \left(\frac{G D_p \eta}{\mu R} \right)^{0.36}$$

In this equation, η is fluidization efficiency defined by

$$\eta = \frac{G - G_e}{G}$$

where G_e is mass velocity of air for the bed expansion.

Most works on the heat transfer in fluidized bed were carried out at temperatures below 200 °C. Only a few works have been carried out at higher temperatures.[7,8] Fluidized bed reactors used in the process of extractive metallurgy are, on the other hand, usually operated at higher temperature. In this connection, this work aims to obtain the heat transfer coefficient at the temperature between 500° and 800 °C and to compare the results obtained with those obtained at lower temperatures.

2. Heat Balance

Quartz and fused alumina were used in this work as the fluidized particles. They were fluidized in the air stream. Heat is supplied to this fluidized bed by a nichrome heater which surrounds the tube wall. At a steady state, therefore, the amount of
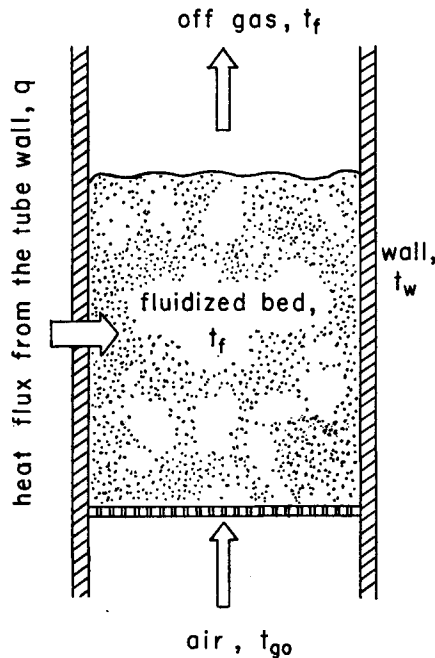

Fig. 1. Heat flow in fluidized bed

heat supplied to the fluidized bed from the heater through the tube wall is equal to the amount of heat consumed in heating the air stream during its ascent through the fluidized bed. This heat flow in the fluidized bed is illustrated in Fig. 1.

In order to establish the heat balance equation with regard to the fluidized bed, the following assumptions were made.

(1) Heat transfer from the distributor located at the bottom of the fluidized bed and from the upper part of the tube wall above the bed surface to the fluidized bed is omitted.

(2) Size of fluidized particles is so small that the temperature profile within the particles is uniform.

(3) Air stream blown into the fluidized bed from the bottom is rapidly heated in the lower part of the bed and the air and particles are in thermal equilibrium in the upper part of the fluidized bed. Temperature in this portion is denoted by $t_f(=t_g=t_p)$.

(4) Owing to the vigorous motion of fluidized particles, temperature of the particles is uniform in both lateral and vertical directions throughout the fluidized bed.

Heat balance with regard to the fluidized bed at the steady state is represented by,

$$h_w A_w (t_w - t_f) - \int_{t_{go}}^{t_f} v\rho_g C_g \, dt = 0 \tag{1}$$

The symbol A_w in this equation represents the inner surface area of the fluidization tube subjected to the heat transfer from the wall to the fluidized bed. It is

$$A_w = \pi D_t L_f \tag{2}$$

From Eq. (1), the heat transfer coefficient between the fluidized bed and the tube wall can be calculated by,

$$h_w = \frac{\int_{t_{go}}^{t_f} v\rho_g C_g \, dt}{A_w (t_w - t_f)} \tag{3}$$

3. Experimental

3.1 Apparatus

Figure 2 demonstrates a schematic illustration of the fluidization apparatus. Fluidization tube is made of 61 mm ID and a 1280 mm long 18–8 stainless steel tube in which the upper and the lower fluidized beds are installed. The upper or main

A Blower
B Rotameter(30-150cc/sec)
C Orifice meter
     (150-900 cc/sec)
D Orifice meter
     (800-2600 cc/sec)
E Manometer
F Fluidization tube
G Furnace
H Distributor
I Main fluidized bed
J Lower fluidized bed
K Aeropak thermocouple
L Cold junction
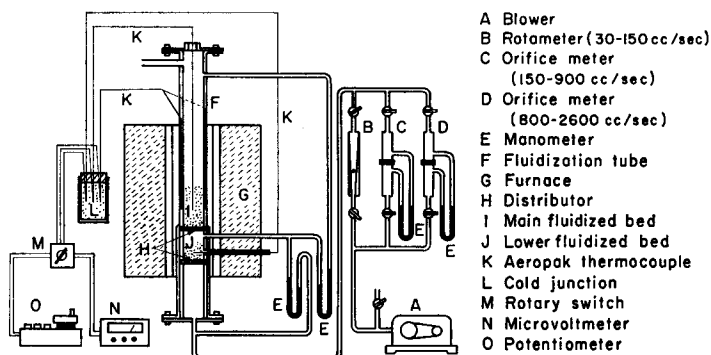M Rotary switch
N Microvoltmeter
O Potentiometer

Fig. 2. Apparatus

fluidized bed is used for measuring the heat transfer coefficient and the lower bed serves for preheating the air stream. The temperature of this lower bed can be regarded as the temperature of the air stream blown into the main fluidized bed, t_{go}.

The distributor at the bottom of main fluidized bed consists of a 300 mesh stainless steel screen sandwiched between two 1.0 mm thick 18–8 stainless steel plates perforated with 3.5 mm D holes spaced on a 7.0 mm triangular pitch. The distributor of the lower fluidized bed is of similar construction, except for the stainless steel plates with 2.0 mm D holes.

The fluidization tube is installed within a nichrome resistance furnace whose lower, middle and upper parts are separately energized and controlled in order to maintain the tube wall at a uniform temperature. The flow rate of air stream is metered with a rotameter or with orifice meters.

The temperature of the tube wall, t_w, and of the upper and the lower fluidized beds, t_f and t_{go}, respectively, are measured by 1.6 mm OD Aeropak chromel-alumel thermocouples. For measuring t_w, four thermocouples are inserted into 4.0 mm wide and 2.5 mm deep vertical grooves along the outer surface of the fluidization tube. Four grooves are cut at a right angle with each other and they are covered with 1.0 mm thick 18–8 stainless steel plates in order to intercept the thermal radiation from the heater to the thermocouples.

The inlet gas temperature, t_{go}, is measured with a thermocouple inserted into the lower fluidized bed through a side tube welded to the fluidization tube. Another thermocouple is lowered from the top of the fluidization tube into the main fluidized bed in order to measure the bed temperature, t_f, and its e.m.f. is measured with a potentiometer. The thermocouples for measuring t_w and t_{go} are differentially connected with the thermocouple of t_f and their differential e.m.f. is measured by a microvoltmeter.

The bed height, L_f, is estimated from the relationship between the pressure in

the fluidized bed and the height above the distributor. Pressure is measured by a 10 mm OD quartz tube manometer inserted from the top of fluidization tube into the bed.

3.2 Material

Quartz and fused alumina particles of 16 to 28, 35 to 42 and 60 to100 mesh sizes were prepared as the fluidized material. The minimum fluidization velocity, u_{mf}, of these particles was measured at 20 °C and listed in Table 1. The heat content per unit volume and the specific gravity of these particles are summarized in Table 2. Heat content of a single fused alumina particle is about 1.5 times larger than that of quartz particles of the same size. This is the reason why these two kinds of particles were chosen as the fluidized material in this work.

Table 1. Minimum fluidization velocity

Particles	Size (mesh)	u_{mf} at 20°C (cm/sec)
Quartz	16–28	26.5
	35–42	21.2
	60–100	4.6
Fused alumina	35–42	36.0
	60–100	12.0

Table 2. Physical Properties of particles

Temperature (°C)		500	650	800
Heat content, C_p [12] (Kcal/m^3·°C)	Quartz	773.1	705.3	741.4
	Fused alumina	1097.5	1160.2	1218.8
Ratio of C_p (–)	$\dfrac{C_p \text{ (alumina)}}{C_p \text{ (quartz)}}$	1.42	1.60	1.64
Specific gravity [13] (g/cm^3 at 25°C)	Quartz		2.64	
	Fused alumina		3.99	

Table 3. Size of fluidized particles employed

Lower fluidized bed		Main fluidized bed	
Particles	Size (mesh)	Particles	Size (mesh)
Activated alumina	28–32	Quartz	16–28
	28–32		35–42
	42–48		60–100
Fused alumina	42–48	Fused alumina	35–42
	60–100		60–100

Activated alumina or fused alumina particles were used as the fluidized particles in the lower fluidized bed. Their size is shown in Table 3. The minimum fluidization velocities of these particles in the lower bed are slightly lower than or equal to the particles in the main fluidized bed.

3.3 Experimental conditions

Effects of the bed temperature, the flow rate of air stream and the size and heat content of particles on the heat transfer coefficient were studied. The levels of these variables examined in this work are listed in Table 4.

Table 4.   Experimental conditions

Amount of fluidized particles		
Quartz: 500g	Fused alumina: 800g	
Particle size		
Quartz: 16–28, 35–42 and 60–100 mesh		
Fused alumina: 35–42 and 60–100 mesh		
Bed temperature: 500°, 650° and 800°C		
Flow rate of air: 2.7–30.0 cm/sec (at 20°C)		

4.   Results and Discussion

An example of the temperature profile along the height of fluidization tube is illustrated in Fig. 3. The bed temperature, t_f, was kept almost unvaried within the bed height and the variation of wall temperature, t_w, was within $\pm 2.5\,°C$. The mean values of t_f and t_w were used to calculate the heat transfer coefficient.

Figure 4 represents the heat transfer coefficient, h_w, calculated from Eq. (3). It is seen in this figure that h_w increases with the flow rate of air stream and that the effects of bed temperature, kind of particles and particle size on h_w are not clearly observed. The values of h_w obtained in this work are 70 to 800 kcal/m²·hr·°C. These values are of the same magnitude as those obtained at lower temperatures below 200°C.[1,2,3,4]

Since the previous measurements of heat transfer coefficient have been carried out under different experimental conditions, it may not be a proper way to compare the values of h_w themselves. The Reynolds number ($Re = D_p G / \mu$) and the Nusselt number ($Nu = h_w D_p / k_g$) are frequently used to express the correlationship between the fluidizing conditions and the heat transfer coefficient. Figure 5 represents the correlationship between Re and Nu calculated from the data obtained in this work. From this figure, the following regression equation was obtained by the least squares method.
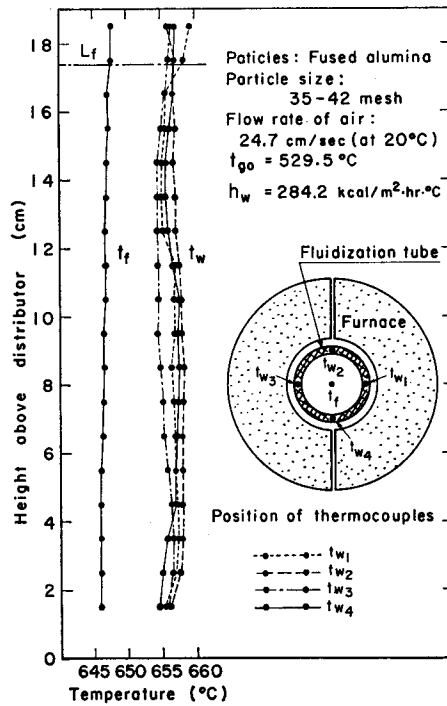
Fig. 3.   An example of temperature profile along the bed height
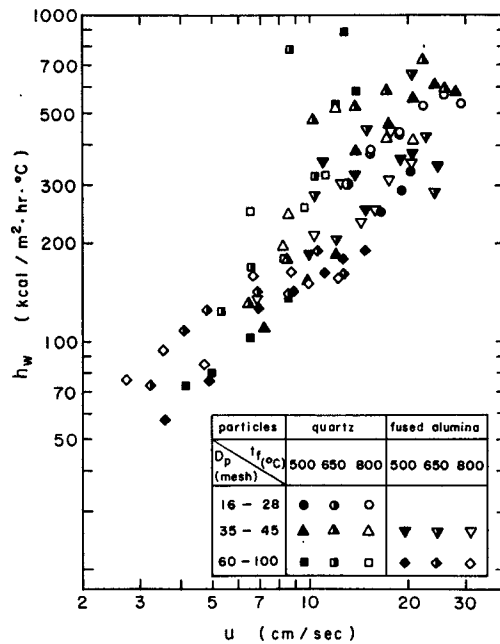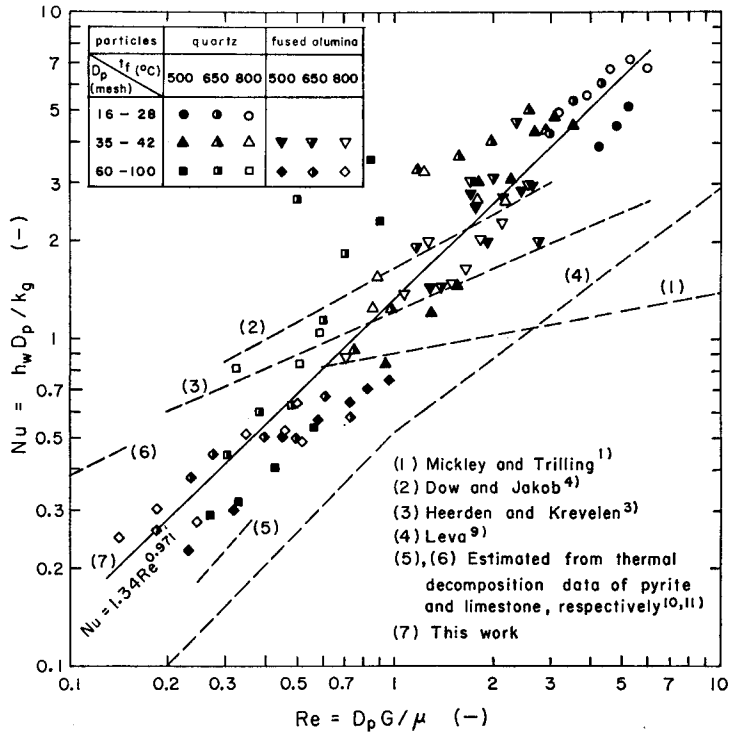

Fig. 4.   Heat transfer coefficient, h_w

Zenjiro Asaki, Takao Nagase, Yasuhiro Awakura, Isao Nakano,
Yasuhiro Fukunaka and Yoshio Kondo

Fig. 5. Correlation between Re and Nu

$$Nu = 1.34\, Re^{0.971} \tag{4}$$

The regression lines calculated from the data of Mickley and Trilling,[1] Dow and Jakob,[4] Heerden and Krevelen[3] and Leva[9] are also illustrated with broken lines in the same figure. Though the regressions of these workers are scattered rather widely, it can be said that the regression obtained in this work coincides fairly well with those obtained at lower temperatures. The broken lines (5) and (6) in this figure represent the correlationships between Re and Nu which were calculated from the thermal decomposition rate of pyrite[10] and limestone[11] in a fluidized bed at 700° to 800°C, respectively. These lines are also within the range of variation of the other broken lines.

Zabrodsky[7] measured the heat transfer coefficient between the vibrating fluidized bed and a solid surface immersed in the bed. He also observed that the heat transfer coefficient obtained between 600° and 700°C coincides well with those obtained at lower temperatures, although the thermal radiation is generally supposed to be another predominant mode of heat transfer at higher temperatures. If the thermal radiation holds an important part in the overall rate of heat transfer between

the fluidized bed and the tube wall, in addition to the convective heat transfer, the values of h_w at higher temperature is thought to be higher than those at lower temperatures. Szekely and Fisher[8] measured the radiative heat transfer coefficient. They installed a transparent glass tube within a graphite cylinder which is heated to about 350 °C. Iron shot, alumina or silicon carbide particles were fluidized in this glass tube. The observed radiative heat transfer coefficient between the graphite cylinder and fluidized bed was 25 to 43 kcal/m²·hr· °C. These values are about one tenth of h_w reported hitherto. Although their experiments were conducted at a fairly lower temperature, the contribution of thermal radiation to the overall rate of heat transfer is again presumed from their experiment to be minor.

It was already mentioned above that the difference between h_w at 500° to 800 °C and those at lower temperature below 200 °C is not significant. From this result, it is acceptable that the contribution of thermal radiation to the overall rate of heat transfer is minor even at the temperature between 500° and 800 °C.

5. Summary

The heat transfer coefficient between fluidized bed and the tube wall, h_w, was measured at elevated temperature between 500° and 800 °C. Quartz and fused alumina particles of 16 to 28, 35 to 42 and 60 to 100 mesh sizes were fluidized by air stream. Fluidization tube is made of 61 mm ID 18–8 stainless steel tube.

The value of h_w was found in the range of 70 to 800 kcal/m²·hr· °C and it increases with the flow rate of air stream. The effects of bed temperature, heat content of particles and particle size on h_w were not significant. The fluidizing conditions and h_w were transformed into the Reynolds number and the Nusselt number and the regression equation (4) was derived. By comparing the results obtained in this work with those obtained at lower temperatures below 200 °C, the difference between both heat transfer coefficients was not significant. This leads to the thought that the effect of thermal radiation on the overall rate of heat transfer at higher temperature is minor.

Notation

g :   acceleration gravity (m/hr²)

h_w :   heat transfer coefficient between fluidized bed and the tube wall (kcal/m²· hr· °C)

k_g :   thermal conductivity of gas (kcal/m·hr· °C)

t_f :   temperature of fluidized bed (°C)

t_g :   gas temperature (°C)

t_{go} : inlet gas temperature (°C)

t_p : particle temperature (°C)

t_w : temperature of fluidization tube wall (°C)

v : flow rate of air (m³/hr)

D_p : particle diameter (m)

D_t : diameter of fluidization tube (m)

C_g : specific heat of air (kcal/kg·°C)

C_p : heat content of particles per unit volume (kcal/m³·°C)

C_s : specific heat of particles (kcal/kg·°C)

G : mass velocity of air (kg/m²·hr)

L_f : height of fluidized bed (m)

R : expansion ratio of fluidized bed (–)

Greek letters

μ : viscosity of air (kg/m·hr)

ρ_g : density of air (kg/m³)

ρ_s : density of particles (kg/m³)

References

1) Mickley, H. S. and C. A. Trilling: Ind. Eng. Chem., 1949, vol. 41, No. 6, pp. 1135–1147
2) Leva, M., M. Weintraub and M. Grummer: Chem. Eng. Progr., 1949, vol. 45, No. 9, pp. 563–572
   Leva, M. and M. Grummer: Chem. Eng. Progr., 1952, vol. 48, No. 6, pp. 307–313
3) Heerden, G., P. Nobel and D. W. Van Krevelen: Chem. Eng. Sci., 1951, vol. 1, No. 2, pp. 51–66: Ind. Eng. Chem., 1953, vol. 45, No. 6, pp. 1237–1242
4) Dow, W. H. and M. Jakob: Chem. Eng. Progr., 1951, vol. 47, No. 12, pp. 637–648
5) Wen, C. Y. and M. Leva: A. I. Ch. E. Journal, 1956, vol. 2, No. 4, pp. 482–488
6) Toomey, R. D. and H. F. Johnstone: Chem. Eng. Progr. Symp. Series, 1953, No. 5, pp. 51–63
7) Zabrodsky, S. S.: Kagaku Kogaku (Chem. Eng., Japan), 1970, vol. 34, No. 6, pp. 594–600 (trans. by R. Toei)
8) Szekely, J. and R. J. Fisher: Chem. Eng. Sci., 1969, vol. 24, pp. 833–849
9) Leva, M.: Proceedings of the General Discussion on Heat Transfer, London, I.M.E., A.S.M.E., 1951, pp. 421–425
10) Yamazaki, S., Z. Asaki and Y. Kondo: Trans. TMS-AIME, 1968, vol. 242, pp. 896–902
11) Asaki, Z.: Dr. Eng. Thesis, 1969, Kyoto Univ.
12) Perry, J. H.: "Chemical Engineers' Handbook" 3rd Ed., 1950, pp. 219–223, McGraw-Hill Book Co., Inc., New York
13) Rikagaku Jiten (Japanese), 1958, p. 54 and 732, Iwanami Book Co., Inc., Tokyo